



A high-order kinetic flux-splitting method for the relativistic magnetohydrodynamics

Shamsul Qamar ^{*}, Gerald Warnecke

Institute for Analysis and Numerics, Otto-von-Guericke University PSF 4120, D-39106 Magdeburg, Germany

Received 16 April 2004; received in revised form 9 September 2004; accepted 4 November 2004
Available online 9 December 2004

Abstract

In this paper we extend the special relativistic hydrodynamic (SRHD) equations [L.D. Landau, E.M. Lifshitz, Fluid Mechanics, Pergamon, New York, 1987] and as a limiting case the ultra-relativistic hydrodynamic equations [M. Kunik, S. Qamar, G. Warnecke, J. Comput. Phys. 187 (2003) 572–596] to the special relativistic magnetohydrodynamics (SRMHD). We derive a flux splitting method based on gas-kinetic theory in order to solve these equations in one space dimension. The scheme is based on the direct splitting of macroscopic flux functions with consideration of particle transport. At the same time, particle “collisions” are implemented in the free transport process to reduce numerical dissipation. To achieve high-order accuracy we use a MUSCL-type initial reconstruction and Runge–Kutta time stepping method. For the direct comparison of the numerical results, we also solve the SRMHD equations with the well-developed second-order central schemes. The 1D computations reported in this paper have comparable accuracy to the already published results. The results verify the desired accuracy, high resolution, and robustness of the kinetic flux splitting method and central schemes.

© 2004 Elsevier Inc. All rights reserved.

MSC: 65M99; 76Y05; 85A30; 85-99

Keywords: Relativistic MHD equations; Kinetic schemes; MUSCL-type reconstruction; Conservation laws; Hyperbolic systems; Discontinuous solutions

1. Introduction

The numerical study of the evolution of multidimensional relativistic flows turns out to be a topic of crucial interest in, at least, two different scientific fields: nuclear physics for studies of the properties of

^{*} Corresponding author. Tel: +49 391 6712027/39 16 71277; fax: +49 391 6718073.

E-mail addresses: shamsul.qamar@mathematik.uni-magdeburg.de (S. Qamar), gerald.warnecke@mathematik.uni-magdeburg.de (G. Warnecke).

the equation of state for nuclear matter via comparison of simulations and experiments of heavy ions collisions and in relativistic astrophysics. The field of numerical astrophysics is recently undergoing an extraordinary development after important efforts in building up robust codes able to describe many different astrophysical scenarios. Astrophysical sources of high-energy radiation and particles involve the presence of relativistic motions in magnetized plasmas. For example, the radio emission from extra galactic jets, especially from the terminal radio lobes, or from plerion-like supernova remnants is due to synchrotron radiation produced by relativistic electron spiraling around magnetic field lines, thus indicating the presence of significant magnetic fields. Strong magnetic fields are supposed to play an essential role in converting the energy of accreting material around super-massive black holes at the center of active galactic nuclei (AGNs) into powerful relativistic jets escaping along open field lines, see Begelman et al. [8]. Similar phenomena may be at work in the galactic compact X-ray sources known as microquasars, see Mirabel and Rodrigues [26]. The other sources of astrophysical phenomena involving magnetic field are accretion into compact objects, collision of compact objects, stellar core collapse and recent models of gamma-ray bursts (GRBs), see Mészáros and Rees [27]. Thus, due to the extreme complexity and richness of the possible effects arising in relativistic plasma physics, the improvement in the efficiency of both relativistic hydrodynamics (RHD) and relativistic magnetohydrodynamics (RMHD) codes becomes necessary.

In recent years, the development of classical MHD codes has attracted much attention. This attention is very natural and necessary since there are several phenomena in astrophysics that require magnetohydrodynamic treatment. Most of the authors considered Godunov-type schemes for this purpose that were found to be very useful here. Early numerical methods were based on a flux corrected transport (FCT) formulation [12] or on artificial viscosity formulations, see Evans and Hawley [15] as well as Stone and Norman [32]. More recently, the need for robustness and reliability in MHD simulations led several authors to formulate numerical MHD schemes that were based on high-order Godunov-type schemes. Several efforts along these lines can be found in the work of Balsara [5,7], Dai and Woodward [11], Londrillo and Del Zanna [23], Roe and Balsara [29], and Ryu et al. [30].

There exist several astrophysical sources of high-energy radiation and particles that involve the presence of relativistic motions in magnetized plasma. During last decade several upwind high-resolution shock-capturing (HRSC) schemes, which were originally derived for the non-relativistic flows, were also applied to RHD and RMHD equations too. These schemes achieve both high accuracy in smooth regions of the simulated flow and sharp discontinuous profiles in the shocks, for example Aloy et al. [4], Balsara [6], Donat and Marquina [13], Eulderink and Mellema [14], Martí and Müller [24,25], Schneider et al. [31], and Del Zana et al. [35,36].

On the other hand, Kunik et al. [18–20] have used kinetic schemes in order to solve the relativistic Euler equations. These relativistic Euler equations result directly from the moments of the relativistic Jüttner equilibrium phase density [17] without taking any approximations. In these papers, we have derived the ultra-relativistic and general form of special relativistic Euler equations. The general form of special relativistic Euler equations covers the whole range from classical to the ultra-relativistic Euler equations. The ultra-relativistic limit can be obtained in the limit of very small particles rest mass or very high temperature. Mathematically the limit of very small rest mass is very easy. We have used the same limit in our paper [18] in order to get the ultra-relativistic phase density from the general phase density. Apart from the above mentioned regimes the ultra-relativistic phase density is not justified because it will not recover the correct constitutive relations. In this paper we will also extend the ultra-relativistic Euler equations as a special case to the ultra-relativistic MHD. As mentioned before, these Euler equations have a kinetic phase density which is a simplified form of the general Jüttner [17] phase density in the ultra-relativistic limit.

The construction of gas-kinetic scheme for the classical MHD equations began with Croisille et al. [10], where a MHD kinetic flux-vector splitting (KFVS) solver was obtained by simply extending the KFVS flux function of the classical Euler equations. The above MHD KFVS scheme is very robust and reliable, but overdiffusive, especially in the contact discontinuity regions, see [13]. Recently, Xu [34] as well as Tang and

Xu [33] have constructed a new BGK-type Kinetic flux splitting method which accounts for the particle collisions at the cell interface. This method was also used by Kunik et al. [20] in order to solve ultra-relativistic Euler equations. The main advantage of the kinetic schemes over other schemes is that kinetic schemes ensures the positivity of pressure and energy density. Furthermore, the kinetic approach is more close to the physics of the given RMHD system.

In this paper we extend the BGK-type KFVS scheme to the special relativistic magnetohydrodynamics (SRMHD) by using the approach of Xu [34] which he used for the classical MHD equations. The scheme is based on the BGK-type formulation, the KFVS SRMHD solver is generalized by including particle collisions. As a result the new scheme reduces the numerical dissipation significantly and gives a more accurate representation of wave interactions. In contrast to the classical case there are several difficulties in solving the SRMHD equations. To obtain the primitive variables from the conserved variable is not as straight forward as in classical MHD case. We will use the idea of Del Zanna et al. [36] in order to obtain the primitive variables from the conserved variables. For the reader's convenience we will also give a short introduction of the special relativistic Euler equations as well as kinetic phase density and its moments. Our model for SRMHD consists of special relativistic Euler equations [21] or as a special case the ultra-relativistic Euler equations [18], which are coupled with usual Maxwell equations, as we know that Maxwell equations are inherently relativistic. In the relativistic MHD case the CFL condition is very simple. Every signal is bounded by the speed of light, therefore it is natural to take $\Delta t = \Delta x/2$. Here Δt is the time step and Δx is the cell width in the 1D spatial domain.

For the direct comparison of the kinetic method results, we also solve the SRMHD equations by using central schemes of Nessyahu and Tadmor [28]. These central schemes are based on the evolution of cell averages over staggered grids. Central schemes eliminate the need for a detailed knowledge of the eigenstructure of the Jacobian matrix. Instead of (approximate) Riemann solvers which are the building blocks of upwind schemes, simple quadrature formulae are used for the time evolution of central schemes. This approach not only saves the costly characteristic decomposition of the Jacobians, but in fact, it allows us to completely avoid the costly evaluation of 7×7 Jacobian matrix in one-space dimension. The resulting central schemes are black-box, Jacobian-free MHD solvers whose sole input is the computed MHD fluxes. Despite of their simplicity these central schemes are able to resolve accurately the complex structure of 1D waves. We demonstrate this with a series of numerical simulations.

This paper has seven sections. In Section 2, we give a brief introduction to special relativistic kinetic theory and special relativistic hydrodynamics (SRHD). In Section 3, we derive relativistic MHD equations which we have to be solved by kinetic and central schemes. In Section 4, we construct kinetic flux splitting method in one space dimension for the solution of relativistic MHD equations. In Section 5, we give a brief introduction to central schemes. Section 6, is dedicated to the numerical test computations. Lastly in Section 7, we give conclusion and remarks.

2. The special relativistic hydrodynamics

Before going to the SRMHD, we first introduce the relativistic kinetic theory and the special relativistic Euler equations. For further details about it the reader is referred to [18,19,21].

The coordinates with respect to a fixed reference frame are given by the four-vector x^μ , $\mu \in \{0, 1, 2, 3\}$, where $x^0 = t$ is the observer time. The three-vector $\mathbf{x} = x^i$, $i \in \{1, 2, 3\}$, denotes the spatial coordinates of any event x^μ . For simplicity we set $c = \hbar = k_B = 1$. Furthermore, we assume that the metric tensor $g_{\mu\nu}$ is given by a diagonal matrix $g_{\mu\nu} = g^{\mu\nu} = \text{diag}(-1, 1, 1, 1)$.

The four-momentum of the gas particles $q^\mu = (q^0, \mathbf{q})$ with $\mathbf{q} = q^i$, $i \in \{1, 2, 3\}$ is a kinetic variable. However, not all components of the four-momentum are independent, because

$$q^\mu q_\mu = -m^2, \quad (1)$$

where m is the rest mass of the particles. The invariant volume element $d\omega$ of the momentum space is given by

$$d\omega = \frac{1}{q^0} dq^1 dq^2 dq^3 = \frac{1}{q^0} d^3q. \quad (2)$$

The phase density $f(x^\mu, q^\mu) \equiv f(t, \mathbf{x}, \mathbf{q})$ gives the number density of particles in the element $d\omega$ at x^μ .

Next we introduce the macroscopic four-velocity u^μ by

$$u^\mu = \frac{1}{\rho} N^\mu, \quad \rho = \sqrt{-N^\nu N_\nu}, \quad (3)$$

so that $u^\mu u_\mu = -1$ and ρ is a particle density. The fluid velocities v^i are given by

$$u^\mu = \gamma(1, v^i), \quad \gamma = u^0 = \frac{1}{\sqrt{1 - \mathbf{v}^2}}, \quad i = 1, 2, 3, \quad (4)$$

where γ is called the Lorentz factor.

Using the Einstein summation convention the equations describing the motion of a relativistic fluid are given by the five conservation laws:

$$\partial_\mu N^\mu = 0, \quad \partial_\mu T^{\mu\nu} = 0. \quad (5)$$

Here, N^μ is a particle density four-vector and $T^{\mu\nu}$ is energy momentum tensor. These tensors are given by

$$N^\mu = \rho u^\mu \quad \text{and} \quad T^{\mu\nu} = (e + p)u^\mu u^\nu + pg^{\mu\nu}, \quad (6)$$

where ρ is rest mass density, p is pressure and e is internal energy. In order to close the system we have the following relation for the energy density

$$e = \rho + \frac{p}{\Gamma - 1}, \quad (7)$$

where Γ is adiabatic index, and $\Gamma = \frac{5}{3}$ in the mildly relativistic case, while $\Gamma = \frac{4}{3}$ in the ultra-relativistic case. Also in the ultra-relativistic case the rest mass density in the (7) is zero hence we get $e = 3p$ in the ultra-relativistic case.

In order to correctly recover the constitute relations (6), we have to modify the ultra-relativistic phase density and its moments, see our papers [18,19]. This ultra-relativistic phase density was obtained from the Jüttner phase density [17] in the ultra-relativistic limit [18]. In the ultra-limit the rest mass is zero, i.e., $m = 0$, so that

$$q_0 \equiv |\mathbf{q}| \quad \text{and} \quad d\omega = \frac{d^3q}{|\mathbf{q}|}. \quad (8)$$

The modified phase density is given by

$$f_J(\rho, T, \mathbf{u}, \mathbf{q}) = \frac{\rho\lambda^3}{8\pi} \exp(\lambda u_\mu q^\mu) = \frac{\rho\lambda^3}{8\pi} \exp\left[-\lambda|\mathbf{q}|\gamma\left(1 - \mathbf{v} \cdot \frac{\mathbf{q}}{|\mathbf{q}|}\right)\right]. \quad (9)$$

Here, $\lambda = 4\rho/(e + p)$ is the normalization factor. The only modification we made in the phase density is the change of the normalization factor λ . Since in the ultra case $e = 3p$, therefore we get back the normalization factor $\lambda = 1/T$ in the ultra-limit, where T denotes the temperature which is defined by $T = p/\rho$. Next the modified moments of the above phase density are given as

$$N^\mu = N^\mu(t, \mathbf{x}) = \int_3 q^\mu f(t, \mathbf{x}, \mathbf{q}) \frac{d^3 q}{|\mathbf{q}|}, \quad (10)$$

$$T^{\mu\nu} = T^{\mu\nu}(t, \mathbf{x}) = \int_3 (q^\mu q^\nu - \delta g^{\mu\nu}) f(t, \mathbf{x}, \mathbf{q}) \frac{d^3 q}{|\mathbf{q}|}, \quad (11)$$

where

$$\delta = \frac{e - 3p}{2\rho\lambda}. \quad (12)$$

The only modification is the additional term in the energy momentum tensor, i.e., the term $\delta g^{\mu\nu}$. The modified moments (10) and (11) are able to recover the constitutive relations (6). However, the constitutive relations (6) are still the limiting case of the general constitutive relations given in [19]. In [19] the phase density for the general constitutive relations has $M(\beta)$ as normalization function which is expressed by using Bessel functions. For the ultra-case the term $\delta g^{\mu\nu}$ is identically zero and we get back the moments for the ultra-case [18]. Furthermore, we are able to obtain an important reduction of the above moment integrals which is presented in the Appendix A.

3. Ideal SRMHD equations

Here we will use the same notations which were used in the previous section for the SRHD equations. The modifications needed to take electromagnetic forces into account are, like in classical MHD, the inclusion of extra terms in the energy–momentum conservation law and a new equation for the magnetic field, to be derived from the Maxwell equations. Our derivation follows the notations used in Anile [1], Balsra [6] and del Zanna et al. [36].

In order to get the SRMHD equation we have to add the electromagnetic contribution to the energy momentum tensor. Therefore, the constitutive relations (6) become

$$N^\mu = \rho u^\mu \quad \text{and} \quad T^{\mu\nu} = (e + p)u^\mu u^\nu + pg^{\mu\nu} + F_\alpha^\mu F^{\nu\alpha} - \frac{1}{4}g^{\mu\nu} F_{\alpha\beta} F^{\alpha\beta}, \quad (13)$$

where we have assumed that $4\pi \rightarrow 1$. Here $F^{\mu\nu}$ denotes the antisymmetric electromagnetic field tensor which satisfies the Maxwell equations

$$\partial_\mu F^{\mu\nu} = -J^\nu, \quad \partial_\mu F^{*\mu\nu} = 0, \quad (14)$$

where J^ν is the four-current containing the source terms, constrained by the condition $\partial_\mu J^\mu = 0$. Here $F^{*\mu\nu} = \frac{1}{2}\epsilon^{\mu\nu\alpha\beta} F_{\alpha\beta}$ is called dual of $F^{\mu\nu}$, where $\epsilon^{\mu\nu\alpha\beta}$ is the Levi–Civita alternating pseudo-tensor¹. Note that

¹ $\epsilon^{\mu\nu\alpha\beta} = \begin{cases} +1 & \text{if } \mu\nu\alpha\beta \text{ is an even permutation of } 0123, \\ -1 & \text{if } \mu\nu\alpha\beta \text{ is an odd permutation of } 0123, \\ 0 & \text{otherwise.} \end{cases}$

$$F^{\mu\nu} = \begin{pmatrix} 0 & E_1 & E_2 & E_3 \\ -E_1 & 0 & B_3 & -B_2 \\ -E_2 & -B_3 & 0 & B_1 \\ -E_3 & B_2 & -B_1 & 0 \end{pmatrix}, \quad (15)$$

which means that

$$F^{0i} = E_i, \quad F^{ij} = \epsilon^{ijk} B_k \quad \text{for } i, j, k = 1, 2, 3, \quad i \neq k, \quad j \neq k. \quad (16)$$

Similarly, $F^{*0i} = B_i$, $F^{*ij} = -\epsilon^{ijk} E_k$. Here, B_i and E_i denote the components of the magnetic field and electric field, respectively.

For an infinitely conducting (perfect MHD) fluid, the electric field in the fluid's frame must vanish [22], i.e.,

$$F^{\mu\nu} u_\nu = 0. \quad (17)$$

This corresponds to the usual MHD condition $\mathbf{E} + \mathbf{v} \times \mathbf{B} = 0$. Note that the other approximation needed to derive the classical MHD equations, namely to neglect the displacement current is not imposed in RMHD. This implies that the current, to be measured from (14), now depends on the time derivative of the electric field too: $\mathbf{J} = \nabla \times \mathbf{B} - \partial_t \mathbf{E}$.

The equations written so far are not easily compared with their MHD equivalent, due to the presence of the electromagnetic tensor and of its dual, both containing the electric field. However, due to Eq. (18), E may be substituted everywhere by defining the electromagnetic induction four-vector as $b^\mu = F^{*\mu\nu} u_\nu$, that allows to write the electromagnetic tensor in terms of u^μ and b^μ alone, i.e.,

$$F^{\mu\nu} = \epsilon^{\alpha\beta\mu\nu} b_\alpha u_\beta. \quad (18)$$

The component of the magnetic field four-vector are

$$b^\mu = [\gamma(\mathbf{v} \cdot \mathbf{B}), \mathbf{B}/\gamma + \gamma(\mathbf{v} \cdot \mathbf{B})\mathbf{v}]. \quad (19)$$

To ensure that the electric field in the plasma's rest frame is zero it has to satisfy the constraint

$$b^\mu u_\mu = 0. \quad (20)$$

The above constraint and the relation $u^\mu u_\mu = -1$ implies that $|\mathbf{b}| = b_\mu b^\mu > 0$, hence b^μ is a space-like vector with

$$|\mathbf{b}|^2 = \mathbf{B}^2/\gamma^2 + (\mathbf{v} \cdot \mathbf{B})^2. \quad (21)$$

Due to the above definitions, the complete set of SRMHD equations becomes

$$\begin{aligned} \partial_\mu(\rho u^\mu) &= 0, \\ \partial_\mu[(e + p) + |\mathbf{b}|^2] u^\mu u^\nu - b^\mu b^\nu + (p + |\mathbf{b}|^2/2) g^{\mu\nu} &= 0, \\ \partial_\mu(u^\mu b^\nu - u^\nu b^\mu) &= 0. \end{aligned} \quad (22)$$

The first equation represent the mass conservation, the second one is energy–momentum conservation and the last one is a magnetic induction equation. We can get back our SRHD equations by simply letting $b^\mu = 0$. In order to learn about the characteristic structure of the 1D RMHD system, the reader is referred to Anile and Pennisi [1,2].

In what follows we will use $v_{x,y,x}$ interchangeable with $v_{1,2,3}$. Similarly, we will use $B_{x,y,z}$ interchangeable with $B_{1,2,3}$.

For numerical work it is useful to treat the equations on a dimension-by-dimension basis. The presence of an underlying computational grid force one to a dimension-by-dimension view. For x -directional

variation we freeze the y - and z -directional variations. For x -directional variations we see from (22)₃ that the magnetic field component in the x -direction is a constant and does not have any temporal variation. This yields another constraint for x -directional variation. Thus there are only seven equations that need to be evolved in time when considering x -directional variations. In a formal vector notation they can be written as

$$\frac{\partial W}{\partial t} + \frac{\partial F(W)}{\partial x} = 0, \quad (23)$$

where

$$W = \begin{pmatrix} D \\ Q^1 \\ Q^2 \\ Q^3 \\ E \\ B_y \\ B_z \end{pmatrix} = \begin{pmatrix} \rho\gamma \\ (e + p + |\mathbf{b}|^2)\gamma^2 v_x - b^0 b^1 \\ (e + p + |\mathbf{b}|^2)\gamma^2 v_y - b^0 b^2 \\ (e + p + |\mathbf{b}|^2)\gamma^2 v_z - b^0 b^3 \\ (e + p + |\mathbf{b}|^2)\gamma^2 - (p + |\mathbf{b}|^2/2) - (b^0)^2 \\ B_y \\ B_z \end{pmatrix} \quad (24)$$

and

$$F(W) = \begin{pmatrix} \rho\gamma v_x \\ (e + p + |\mathbf{b}|^2)\gamma^2 v_x^2 + (p + |\mathbf{b}|^2/2) - (b^1)^2 \\ (e + p + |\mathbf{b}|^2)\gamma^2 v_x v_y - b^1 b^2 \\ (e + p + |\mathbf{b}|^2)\gamma^2 v_x v_z - b^1 b^3 \\ (e + p + |\mathbf{b}|^2)\gamma^2 v_x - b^0 b^1 \\ B_y v_x - B_x v_y \\ B_z v_x - B_x v_z \end{pmatrix} = 0. \quad (25)$$

In order to get primitive variables from the conserved variables we use the idea of Del Zanna et al. [36]. The vector \mathbf{Q} becomes

$$\mathbf{Q} = (U + \mathbf{B}^2)\mathbf{v} - (\mathbf{v} \cdot \mathbf{B})\mathbf{B}, \quad (26)$$

and by taking the projection along \mathbf{B} we can obtain

$$S \equiv (\mathbf{Q} \cdot \mathbf{B}) = U(\mathbf{v} \cdot \mathbf{B}), \quad (27)$$

where $U = w\gamma^2$, $w = e + p = \rho + \Gamma_1 p$, and $\Gamma_1 = \Gamma/(\Gamma - 1)$.

A 2×2 system can be obtained by taking the square of (26) and by taking the equation for total energy E :

$$U^2 \mathbf{v}^2 + (2U + \mathbf{B}^2)\mathbf{B}^2 v_{\perp}^2 - \mathbf{Q}^2 = 0, \quad (28)$$

$$U - p + \frac{1}{2}\mathbf{B}^2 + \frac{1}{2}\mathbf{B}^2 v_{\perp}^2 - E = 0, \quad (29)$$

where $\mathbf{B}^2 v_{\perp}^2 \equiv \mathbf{B}^2 \mathbf{v}^2 - (\mathbf{v} \cdot \mathbf{B})^2 = \mathbf{B}^2 \mathbf{v}^2 - S^2/U^2$. If we use the relations

$$\rho = D\sqrt{1 - \mathbf{v}^2}, \quad p = [(1 - \mathbf{v}^2)U - \rho]/\Gamma_1, \quad (30)$$

it comes out that all the quantities appearing in the system are written in terms of the two unknown \mathbf{v}^2 (or equivalently γ) and U . Once these variables are found numerically, the primitive quantities will be easily derived through (30) and by inverting (26), that is,

$$v_k = \frac{1}{U + \mathbf{B}^2} \left(Q_k + \frac{S}{U} B_k \right), \quad k = x, y, z. \quad (31)$$

Note that Eqs. (26)–(30) only work for polytropic gases. In order to bring the system down to just a single non-linear equation, which as to be solved numerically, it is useful to define $\mathbf{B}^2 \mathbf{v}_\perp^2 = T^2 / (U + \mathbf{B}^2)^2$ in Eqs. (28) and (29). Here $T^2 = \mathbf{B}^2 \mathbf{Q}^2 - S^2$ is a new, but given, parameter. Then we write Eq. (29) as a third-order algebraic equation for U with coefficients that depend on \mathbf{v}^2 alone

$$\left[\left(1 - \frac{1 - \mathbf{v}^2}{\Gamma_1} \right) U - E + \frac{\rho}{\Gamma_1} + \frac{\mathbf{B}^2}{2} \right] (U + \mathbf{B}^2)^2 + \frac{T^2}{2} = 0, \quad (32)$$

which can be solved analytically, see Abramowitz and Stegun [3]. Note that the cubic polynomial on the left hand side has a positive local maximum in $U = -\mathbf{B}^2$. Thus, since we know that at least one root must be positive, all the other roots of above equation are actually bound to be real, it was found that the largest one gives the correct results, see Del Zanna et al. [36].

In order to get the ultra-relativistic MHD equations we have to use $e = 3p$, $\Gamma = \frac{3}{4}$, and $\Gamma_1 = 4$ in above equations. Also in the ultra-relativistic MHD case the rest mass density ρ is zero in Eq. (32). The resulting MHD equations are then called ultra-relativistic magnetohydrodynamic (URMHD) equations.

The function $U(\eta)$ with $\eta = \mathbf{v}^2$, is thus available together with its derivatives $U'(\eta)$, so the final step is to apply Newton's method to find the root of $\mathbb{F}(\eta) = 0$, where

$$\mathbb{F}(\eta) = U^2 \eta + (2U + \mathbf{B}^2) \frac{T^2}{(U + \mathbf{B}^2)^2} - \mathbf{Q}^2 \quad (33)$$

and

$$\mathbb{F}'(\eta) = U^2 + 2UU' \left(\eta - \frac{T^2}{(U + \mathbf{B}^2)^3} \right). \quad (34)$$

4. Kinetic flux splitting method

In gas-kinetic theory, the flux is associated with the particle motion across a cell interface. For 1D flow in the x -direction, the particle motion in this direction determines the flux function. Other quantities, such as y -direction velocity, thermal energy, density, magnetic field and pressure can be considered as passive scalars which are transported with the x -direction particle velocity. Normally particles are randomly distributed around the average velocity. From statistical mechanics, the moving particles in the x -direction can be most favorably described by the relativistic Maxwellian (9), i.e., Jüttner phase density. For SRMHD case we will use the same technique which was used by Xu [34] in the case of classical MHD equations. Also we have already used this method in order to derive kinetic flux splitting method for the ultra-relativistic Euler equations [20]. We refer the reader to these references for further details.

The transport of any flow quantity is basically due to the movement of particles. With the phase density f_J in (9), we can split the particles into two groups. One group is moving to the right with $v_x > 0$ and the other group is moving to the left with $v_x < 0$. For the present 1D variation of the SRMHD equations it is sufficient to consider only the 1D phase density. As the normalization factor λ in the reduced moment

integrals (A.3) and (A.4) drops out, therefore we do not need to modify the normalization factor. Before splitting the fluxes we introduce the new coordinates $-1 \leq \xi \leq 1$, $0 \leq \vartheta \leq 2\pi$,

$$\alpha^1 = \xi \quad \alpha^2 = \sqrt{1 - \xi^2} \sin \vartheta, \quad \alpha^3 = \sqrt{1 - \xi^2} \cos \vartheta.$$

Introducing these new coordinates in (A.3)₁ and (A.4) we get in the 1D case

$$\langle u^0 \rangle = 1 = \int_{-1}^1 \frac{1}{2\gamma^2(1 - \xi v_x)^2} d\xi, \quad \langle u^1 \rangle = v_x = \int_{-1}^1 \frac{\xi}{2\gamma^3(1 - \xi v_x)^3} d\xi. \quad (35)$$

The above two moments are sufficient to split all the fluxes. In order to simplify the notation we define

$$\langle u^0 \rangle_+ = \int_0^1 \frac{1}{2\gamma^2(1 - \xi v_x)^2} d\xi, \quad \langle u^0 \rangle_- = \int_{-1}^0 \frac{1}{2\gamma^2(1 - \xi v_x)^2} d\xi. \quad (36)$$

Similarly,

$$\langle u^1 \rangle_+ = \int_0^1 \frac{\xi}{2\gamma^3(1 - \xi v_x)^3} d\xi, \quad \langle u^1 \rangle_- = \int_{-1}^0 \frac{\xi}{2\gamma^3(1 - \xi v_x)^3} d\xi. \quad (37)$$

Here we can see that the resulting splitted moment integrals are free from the normalization factor γ . Also both SRHD [21] and ultra-relativistic Euler equations [18] have the same continuity equation. These two are the main reason to use the above moments for the splitting of both SRHD and ultra-relativistic Euler equations fluxes.

After having the above definitions, we are ready to split the SRMHD flux function (25),

$$F = \begin{pmatrix} \rho\gamma v_x \\ (w + |\mathbf{b}|^2)\gamma^2 v_x^2 + (p + |\mathbf{b}|^2/2) - (b^1)^2 \\ (w + |\mathbf{b}|^2)\gamma^2 v_x v_y - b^1 b^2 \\ (w + |\mathbf{b}|^2)\gamma^2 v_x v_z - b^1 b^3 \\ (w + |\mathbf{b}|^2)\gamma^2 v_x - b^0 b^1 \\ B_y v_x - B_x v_y \\ B_z v_x - B_x v_z \end{pmatrix} = F_f^+ + F_f^-, \quad (38)$$

where $w = e + p$ and

$$F_f^\pm = \langle u^1 \rangle_\pm \begin{pmatrix} \rho\gamma \\ (w + |\mathbf{b}|^2)\gamma^2 v_x \\ (w + |\mathbf{b}|^2)\gamma^2 v_y \\ (w + |\mathbf{b}|^2)\gamma^2 v_z \\ (w + |\mathbf{b}|^2)\gamma^2 \\ B_y \\ B_z \end{pmatrix} + \langle u^0 \rangle_\pm \begin{pmatrix} 0 \\ (p + |\mathbf{b}|^2/2) - (b^1)^2 \\ -b^1 b^2 \\ -b^1 b^3 \\ -b^0 b^1 \\ -B_x v_y \\ -B_x v_z \end{pmatrix}. \quad (39)$$

When we conclude the above splitting of fluxes, the free transport flux for the SRMHD equations at a cell interface becomes

$$F_{i+\frac{1}{2}}^f = F_{i,f}^+ + F_{i+1,f}^-, \quad (40)$$

where “f” is used to denote the above free transport model. The KFVS-type MHD method is very robust, but over diffusive, especially in the case with the coarse mesh. To reduce numerical dissipation Xu [34], in the classical MHD case, implemented a particle collision mechanism in above flux transport process. The idea is to obtain an equilibrium state $\overline{W}_{i+\frac{1}{2}}$ at the cell interface by combining the left and right moving beams and use this state to get an equilibrium flux function $F^c(\overline{W}_{i+\frac{1}{2}})$ through the flux function definition in (38). Using (24), the equilibrium state at the cell interface can be obtained as

$$\overline{W}_{i+\frac{1}{2}} = \begin{pmatrix} \rho\gamma \\ (w + |\mathbf{b}|^2)\gamma^2 v_x - b^0 b^1 \\ (w + |\mathbf{b}|^2)\gamma^2 v_y - b^0 b^2 \\ (w + |\mathbf{b}|^2)\gamma^2 v_z - b^0 b^3 \\ (w + |\mathbf{b}|^2)\gamma^2 - (p + |\mathbf{b}|^2/2) - (b^0)^2 \\ B_y \\ B_z \end{pmatrix} = W_i^+ + W_{i+1}^-, \quad (41)$$

where

$$W_i^\pm = \begin{pmatrix} \rho\gamma\langle u^0 \rangle_\pm \\ (w + |\mathbf{b}|^2)\gamma^2\langle u^1 \rangle_\pm - b^0 b^1\langle u^0 \rangle_\pm \\ [(w + |\mathbf{b}|^2)\gamma^2 v_y - b^0 b^2]\langle u^0 \rangle_\pm \\ [(w + |\mathbf{b}|^2)\gamma^2 v_z - b^0 b^3]\langle u^0 \rangle_\pm \\ [(w + |\mathbf{b}|^2)\gamma^2 - (p + |\mathbf{b}|^2/2) - (b^0)^2]\langle u^0 \rangle_\pm \\ B_y\langle u^0 \rangle_\pm \\ B_z\langle u^0 \rangle_\pm \end{pmatrix}_i. \quad (42)$$

With the above averaged macroscopic variables $\overline{W}_{i+\frac{1}{2}}$, the equilibrium flux can be obtained as

$$F_{i+\frac{1}{2}}^c = F^c(\overline{W}_{i+\frac{1}{2}}) = \begin{pmatrix} \overline{\rho}\overline{\gamma}\overline{v}_x \\ (\overline{w} + |\overline{\mathbf{b}}|^2)\overline{\gamma}^2\overline{v}_x^2 + (\overline{p} + |\overline{\mathbf{b}}|^2/2) - (\overline{b}^1)^2 \\ (\overline{w} + |\overline{\mathbf{b}}|^2)\overline{\gamma}^2\overline{v}_x\overline{v}_y - \overline{b}^1\overline{b}^2 \\ (\overline{w} + |\overline{\mathbf{b}}|^2)\overline{\gamma}^2\overline{v}_x\overline{v}_z - \overline{b}^1\overline{b}^3 \\ (\overline{w} + |\overline{\mathbf{b}}|^2)\overline{\gamma}^2\overline{v}_x - \overline{b}^0\overline{b}^1 \\ \overline{B}_y\overline{v}_x - \overline{B}_x\overline{v}_y \\ \overline{B}_z\overline{v}_x - \overline{B}_x\overline{v}_z \end{pmatrix}, \quad (43)$$

where $\overline{B}_x = B_x$ is constant in 1D case. The final flux function is a combination of non-equilibrium and equilibrium flux functions

$$F_{i+\frac{1}{2}} = \chi F_{i+\frac{1}{2}}^f + (1 - \chi)F_{i+\frac{1}{2}}^c, \quad (44)$$

where χ is an adaptive parameter, see [34]. In the first order scheme χ can be fixed at, say 0.7 or 0.5, in the numerical calculations. Theoretically χ should depend on the real flow situations: in equilibrium and smooth regions, the use of $\chi \sim 0$ is physically reasonable, and in the regions with discontinuities, χ should be close to 1 in order to have enough numerical dissipation to recover smooth shock transition. A possible

choice for η in a high-order scheme is to consider it as a function of the pressure difference, such as the switch function in the JST scheme [16], see Xu [34] for further details.

The integration of (23) over the cell $[x_{i-\frac{1}{2}}, x_{i+\frac{1}{2}}]$ gives the following semi-discrete kinetic upwind scheme:

$$\frac{dW_i}{dt} = -\frac{F_{i+\frac{1}{2}} - F_{i-\frac{1}{2}}}{\Delta x}, \tag{45}$$

where $F_{i+\frac{1}{2}}$ is the fluxes at the cell boundary $x_{i+\frac{1}{2}}$ and is given by (44). Here Δx represent the cell width. The above scheme is only first order accurate in space. To get high-order accuracy, the initial reconstruction strategy must be applied to interpolate the cell averaged variables W_i^n . For example the linear interpolation

$$W(t^n, x) = W_i^n + W_i^x \frac{(x - x_i)}{\Delta x}, \tag{46}$$

can be constructed to approximate the cell averaged variables W_i^n at the beginning of each time step t^n , where W_i^x is approximate slope. The extreme points $x = 0$ and $x = \Delta x$, in local coordinates correspond to the intercell boundaries in general coordinates $x_{i-\frac{1}{2}}$ and $x_{i+\frac{1}{2}}$, respectively. The values W_i at the extreme points are

$$W_i^L = W_i^n - \frac{1}{2} W_i^x, \quad W_i^R = W_i^n + \frac{1}{2} W_i^x. \tag{47}$$

To avoid oscillations in the reconstructed data, the slope W_i^x is obtained from the min-mode limiter as follows:

$$W_i^x = MM \left(\theta \Delta W_{i+\frac{1}{2}}, \frac{\theta}{2} (\Delta W_{i-\frac{1}{2}} + \Delta W_{i+\frac{1}{2}}), \theta \Delta W_{i-\frac{1}{2}} \right).$$

Here, Δ denotes the central differencing, $\Delta W_{i+\frac{1}{2}} = W_{i+1} - W_i$, and MM denotes the min-mode non-linear limiter

$$MM\{x_1, x_2, \dots\} = \begin{cases} \min_i \{x_i\} & \text{if } x_i > 0 \ \forall i, \\ \max_i \{x_i\} & \text{if } x_i < 0 \ \forall i, \\ 0 & \text{otherwise,} \end{cases} \tag{48}$$

where $1 \leq \theta \leq 2$ is a parameter. Based on the above reconstruction, a high spatial resolution kinetic SRMHD solver becomes

$$\frac{dW_i}{dt} = -\frac{F_{i+\frac{1}{2}}(W_{i+1}^L, W_i^R) - F_{i-\frac{1}{2}}(W_i^L, W_{i-1}^R)}{\Delta x}. \tag{49}$$

To improve the temporal accuracy, we use a second-order TVD Runge–Kutta scheme to solve (49). Denoting the right-hand side of (49) as $L(W)$, a second-order TVD Runge–Kutta scheme update W through the following two stages:

$$W^{(1)} = W^n + \Delta t L(W^n), \tag{50}$$

$$W^{n+1} = \frac{1}{2} (W^n + W^{(1)} + \Delta t L(W^{(1)})). \tag{51}$$

5. Central schemes

The intrinsic complexity of the SRMHD equations suggests the class of central schemes as an efficient alternative for the class of upwind schemes, for computing approximate solutions of Eqs. (23)–(25). The

central schemes we use in this paper are based on the evolution of cell averages over staggered grids, see Nessyahu and Tadmor [28]. Central schemes eliminate the need for a detailed knowledge of the eigen-structure of the Jacobian matrix. Instead of (approximate) Riemann solvers as building blocks for upwind schemes, simple quadrature formulae are used for the time evolution of central schemes. This approach not only saves the costly characteristic decomposition of the Jacobians, but in fact, it allows us to completely avoid the costly evaluation of 7×7 Jacobian matrix in one space dimension. The resulting central schemes are black-box, Jacobian-free MHD solvers whose sole input is the computed MHD fluxes. Despite of their simplicity these central schemes are able to resolve accurately the complex structure of 1D waves. We demonstrate this with a series of numerical simulations. Central schemes have the following predictor-corrector form [28]:

$$W_i^{n+\frac{1}{2}} = W_i^n - \frac{\lambda}{2} F^x(W_i), \quad (52)$$

$$\overline{W}_{i+\frac{1}{2}}^{n+1} = \frac{1}{2}(W_i^n + W_{i+1}^n) + \frac{1}{8}(W_i^x - W_{i+1}^x) + \lambda \left[F(W_i^{n+\frac{1}{2}}) - F(W_{i+1}^{n+\frac{1}{2}}) \right], \quad (53)$$

where W_i^n are the cell averaged initial data, while W_i^x and F_i^x are the approximate slopes of the conservative variables and fluxes, respectively. These slopes can be calculated from the same initial reconstruction and min-mode formulae which are given by (46) and (48). Here $\lambda = \Delta t / \Delta x$. For further details about these schemes the reader is referred to the paper of Nessyahu and Tadmor [28].

6. Numerical case studies

In the following we present numerical test cases for the solution of the SRMHD equations in both SRHD and ultra-relativistic cases. For the comparison we give the results of high-order central schemes. In all numerical computation we have used a natural CFL condition $\Delta t = \Delta x / 2$, as every signal is bounded by the speed of light.

6.1. SRMHD equations

In this case the SRMHD equation consist of special relativistic Euler equations of [21] which are coupled with Maxwell equations. All the test cases presented here are the same which were considered in Balsara [6] and Del Zanna et al. [36]. In all the problems given in Table 1 we use $\Gamma = \frac{5}{3}$ which was also used by [6,36] except for the first one where [6] used $\Gamma = 2$. Also for better comparison we use the same 1600 mesh points which were used by [6,36]. We give the results of both kinetic and central schemes. Since in the 1D SRMHD case the solenoidal constraint $\nabla \cdot \mathbf{B} = 0$ is automatically satisfied and transverse magnetic field components behave essentially like the other conservative variables therefore we can directly apply the kinetic method and central schemes as black-box solvers. The shock tube tests shown here illustrate the ability of the both codes to handle degenerate cases where the system is no longer strictly hyperbolic due to the coincidence of two or more eigenvalues. The results also show the ability of the code to separate the various Riemann discontinuities or rarefaction waves, which are more numerous in the magnetized case (up to seven) rather than in the fluid case (just three).

The results related to the first test are shown in Fig. 1. This is a relativistic analog of the Brio and Wu [9] test problem. It shows a left-going fast rarefaction wave, a left-going compound wave, a contact discontinuity, a right-going slow shock and a right going fast rarefaction wave. A modest Lorentz factor with a maximum value of about 1.46 is established indicating that a reasonably relativistic flow has developed. All the waves that developed in this example can be clearly identified. The results obtained from the kinetic

Table 1
Parameters for Riemann problems

Test	ρ	p	v_x	v_y	v_z	B_y	B_z	B_x	t_s
1 L	1.0	1.0	0.0	0.0	0.0	1.0	0.0	0.5	0.4
1 R	0.125	0.1	0.0	0.0	0.0	-1.0	0.0	-	-
2 L	1.0	30.0	0.0	0.0	0.0	6.0	6.0	5.0	0.4
2 R	1.0	1.0	0.0	0.0	0.0	0.7	0.7	-	-
3 L	1.0	1000.0	0.0	0.0	0.0	7.0	7.0	10.0	0.4
3 R	1.0	0.1	0.0	0.0	0.0	0.7	0.7	-	-
4 L	1.0	0.1	0.999	0.0	0.0	7.0	7.0	10.0	0.4
4 R	1.0	0.1	-0.999	0.0	0.0	-7.0	-7.0	-	-
5 L	1.08	0.95	0.4	0.3	0.2	0.3	0.3	2.0	0.55
5 R	1.0	1.0	-0.45	-0.2	0.2	-0.7	0.5	-	-

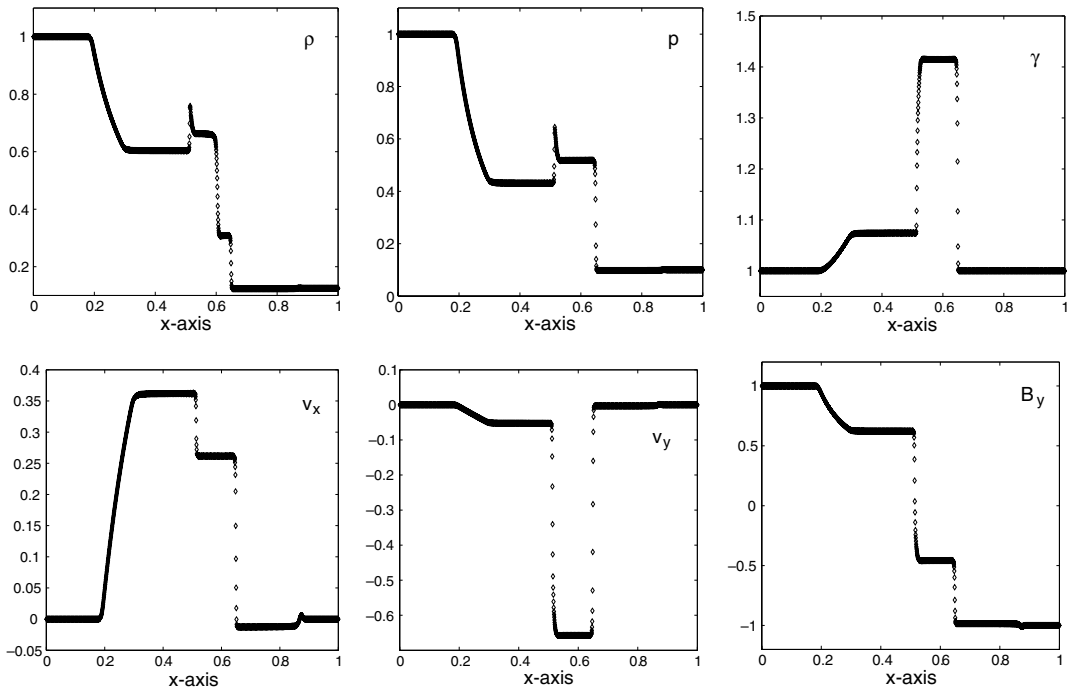
method and central scheme give comparable accuracy to that of [6,36]. We use $\chi = 0.5$ in the kinetic scheme. Both the kinetic and central schemes capture all the waves very perfectly. Although central central schemes are believed to be very diffusive, here we see that the schemes worked very well.

Figs. 2 and 3 are blast wave examples which are again taken from [6]. The first blast wave has a moderate jump, while the second has a large pressure jump of the order 10^4 which produces a relativistic flow with a maximum Lorentz factor of $\gamma = 3.4$. In these cases our results are again comparable that of [6,36]. All the waves that developed in these Riemann problems can be clearly identified. In Fig. 2 we have a left-going fast rarefaction wave, a left-going slow rarefaction wave, a contact discontinuity, a right-going slow shock and a right-going fast shock. The maximum value of the Lorentz factor in this example is 1.36 which indicates that the problem is reasonably relativistic. Fig. 3 shows that a pair of left-going rarefaction waves also appear in this case. The maximum value of the Lorentz factor in this case is 3.4 which indicates a strong relativistic flow. The high Lorentz factor means that the relativistic length-contraction becomes more effective which causes compression of the structures moving to the right when viewed in the laboratory frame which is also our computational grid. As a result we get under-resolved contacts and right-going shocks as compared to Fig. 2. In Fig. 3 the jump in the density pulse obtained from the kinetic scheme, which is up to 8.7, for the parameter $\chi = 0.7$ has a better resolution as compared to the central schemes which is up to 7.8. However, the kinetic scheme does not resolve it as well as in [6,36] with jumps up to 9.5. The same is the case for the y -component for velocity and the magnetic field.

Fig. 4 shows the results of the fourth test case which was proposed by Balsara [6]. The two streams that are approaching each other have an initial Lorentz factor of 22.366. Thus it is a strongly relativistic problem. The initial pressure in the stream is 10^{-6} time smaller than their initial energy density. Two extremely strong fast shock waves are established in the flow, one is flowing to the right and the other to the left. We also see that two slow shocks are established, one of which is right-going and the other is left-going. These are seen to be switch-off slow shocks. Thus it is interesting to observe that the switch-off slow shocks in non-relativistic MHD also have their relativistic analogs. Here we use the diffusive parameter $\chi = 0.7$ in the kinetic scheme in order to reduce the post shock oscillations in the results. Our results are again of comparable accuracy to that of [6,36]. The good performance of our codes demonstrates the robustness and accuracy of the schemes.

Fig. 5 shows a left-going fast shock, a left-going Alfvén wave, a left-going slow rarefaction fan, a contact discontinuity, a right-going slow shock, a right-going Alfvén wave, and a right-going fast shock. We use $\chi = 0.5$ in the kinetic scheme. The results obtained from both central and kinetic schemes have again comparable accuracy to that of [6].

(a) Gas Kinetic method results



(b) Central schemes results

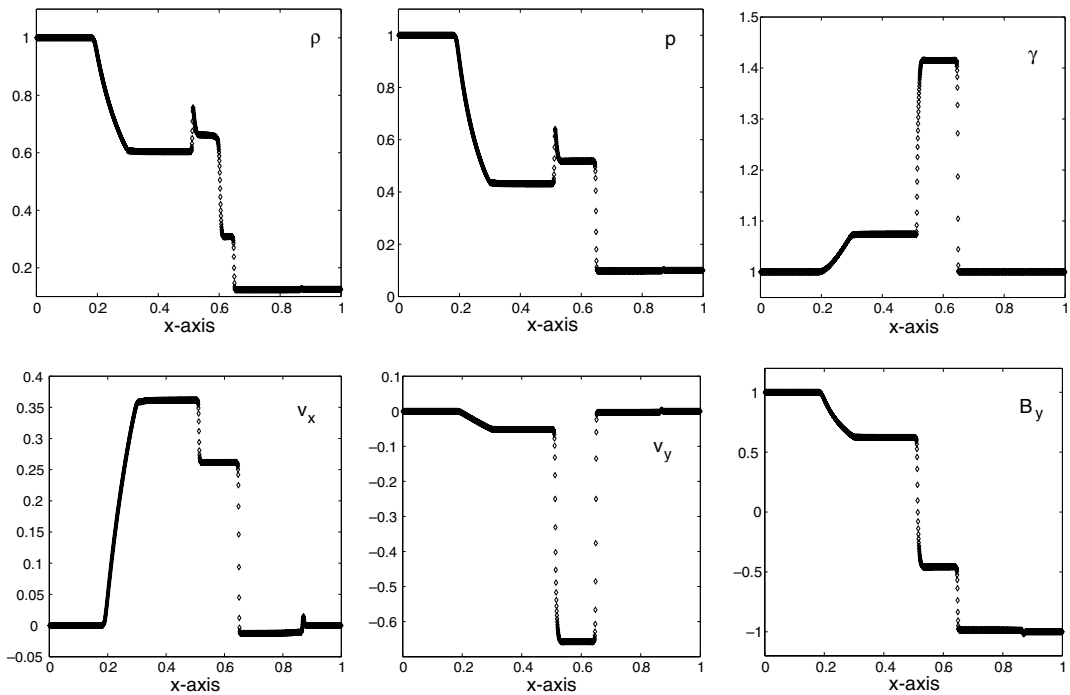
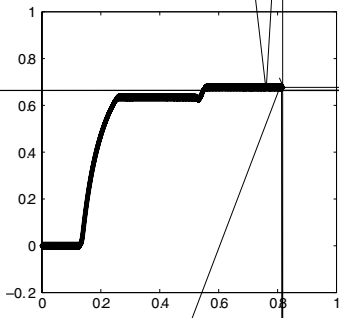
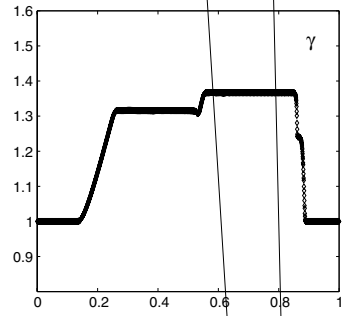
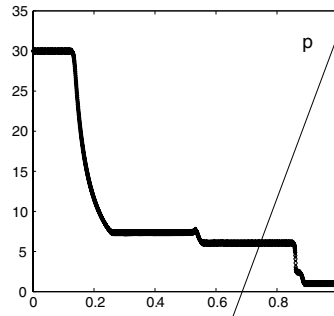
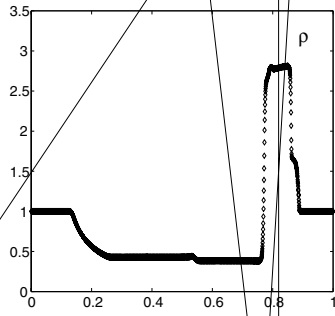
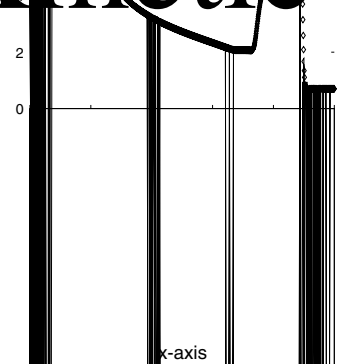
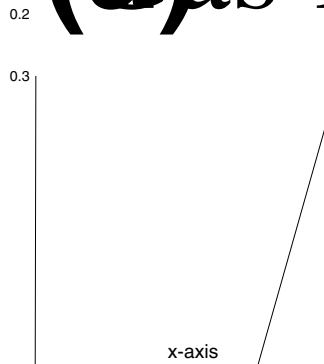
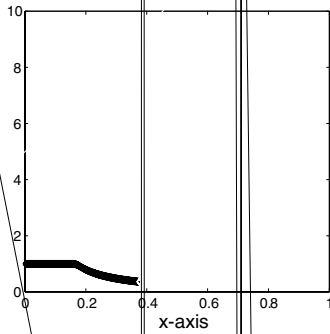


Fig. 1. Results of test 1 at time $t = 0.4$.



S. Qamar G. W. Wood
(a) as Kinetic method



(b) Central schemes

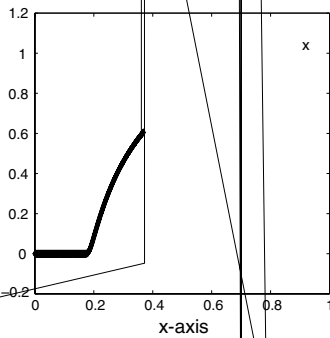
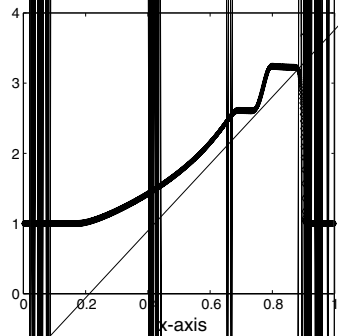
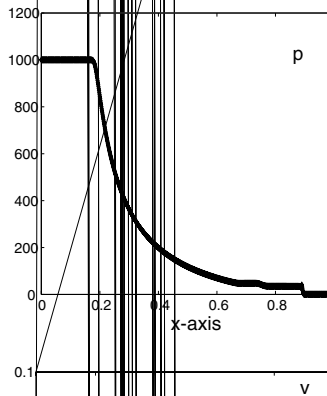
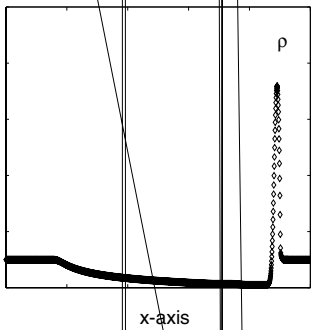
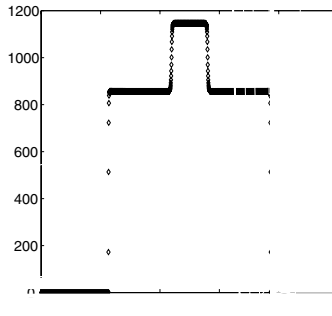
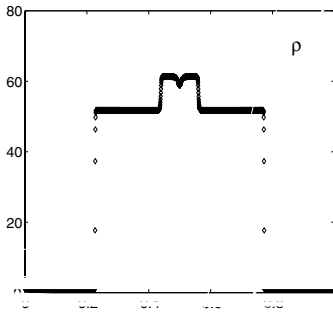


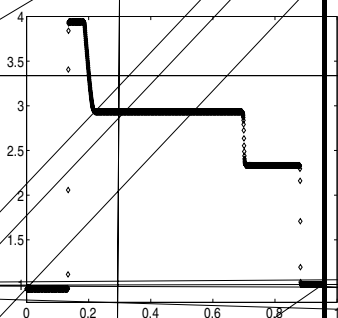
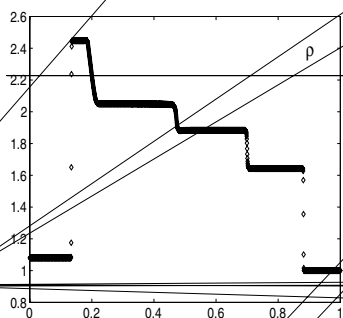
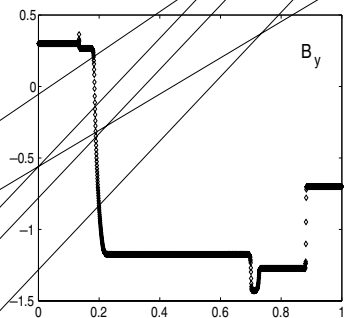
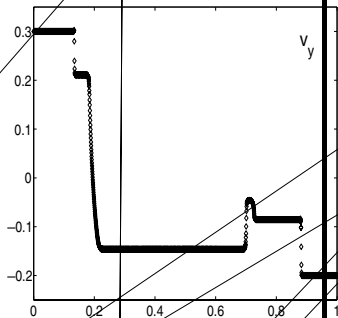
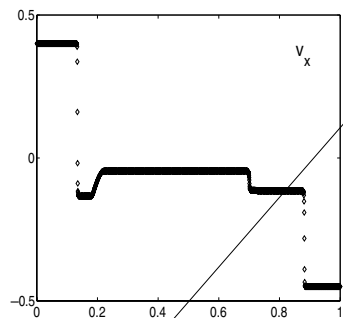
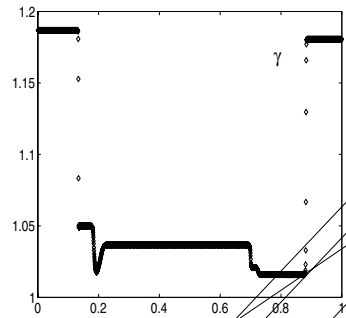
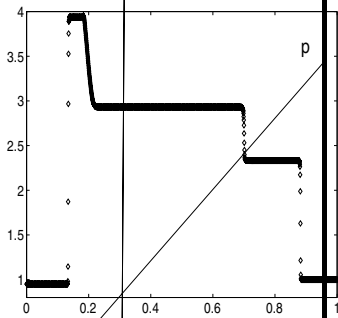
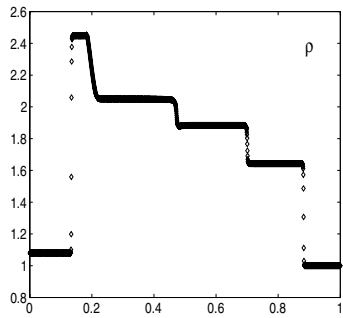
Fig. 3. Results of



v

0





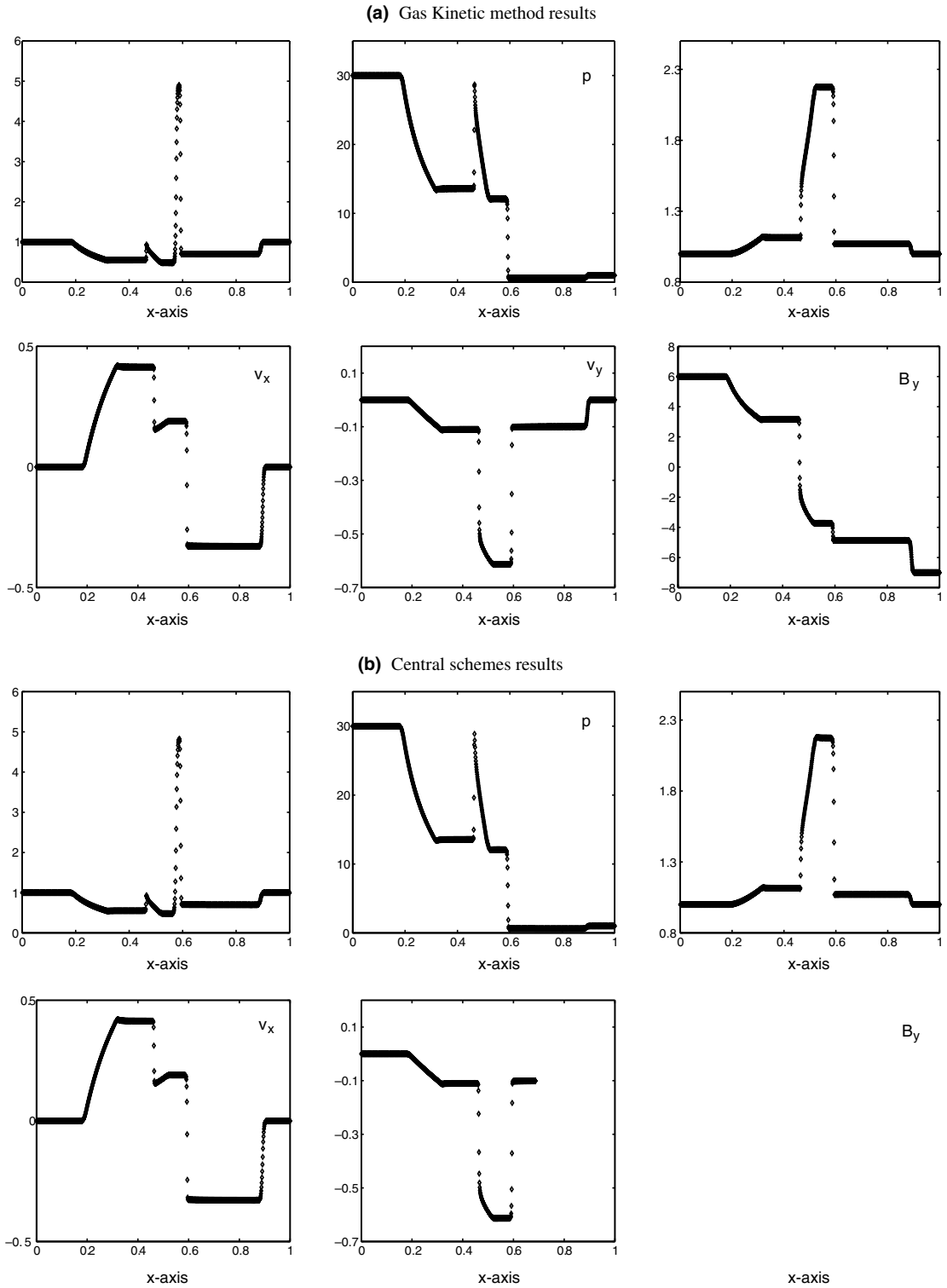
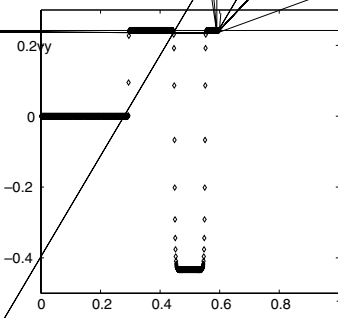
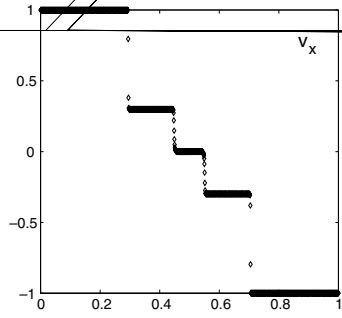
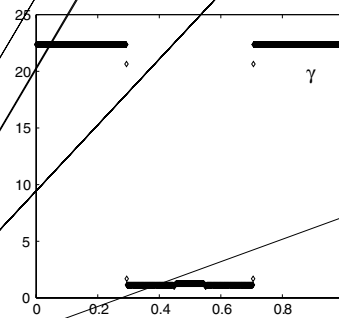
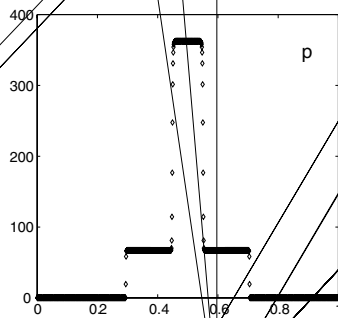
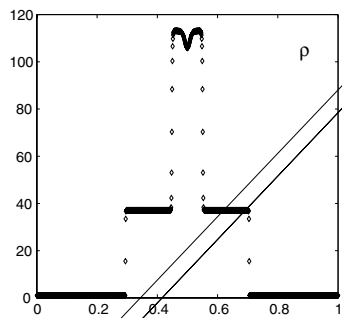
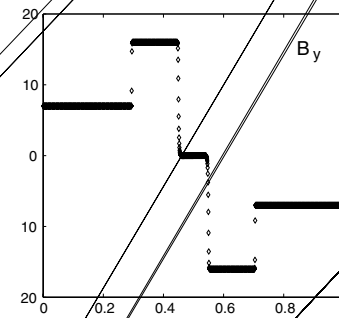
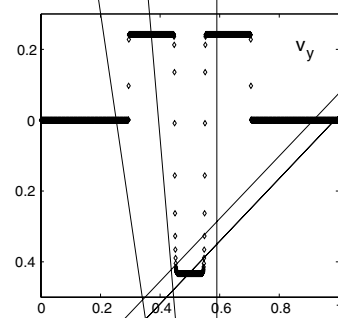
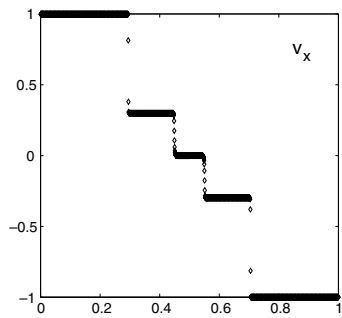
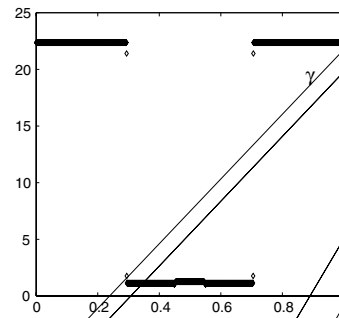
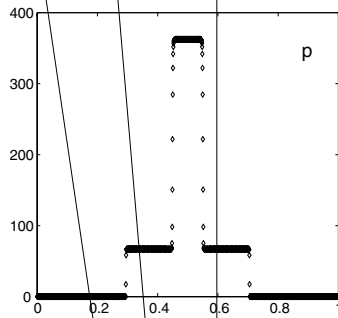
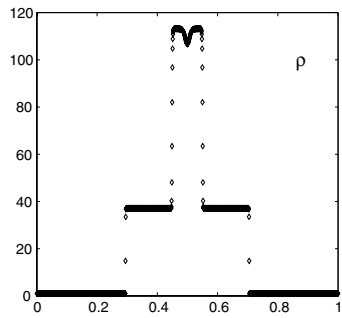


Fig. 6. Results of test 6 at time $t = 0.4$.



6.2. Ultra-relativistic MHD (URMHD) equations

In this case the relativistic MHD equation consist of the ultra-relativistic Euler equations [18,19] which are coupled with Maxwell's equations. Here we consider two test problems. The initial data are the same as in Test 2 and Test 4 of Table 1 for the same final time. Here we use the parameter $\chi = 0.7$ in the kinetic scheme.

Fig. 6 is blast wave examples which is the same as in Test 2 of Table 1. The maximum value of the Lorentz factor in this case is 2.18, while it was 1.36 in the case of Fig. 2. Hence the relativistic length-contraction effects are more pronounced here as compared to Fig. 2 which causes compression of the structures moving to the right when viewed in the laboratory frame which is also our computational grid. As a result we get an under-resolved contact and right-going shocks as compared to Fig. 2. Since the basic equations are different, therefore we can see that both solutions of Figs. 2 and 6 are quite different although both have the same initial data and final time.

Fig. 7 shows the results of the second test case in ultra-MHD case. The initial data are the same as in Test 4 of Table 1. If we compare these results to that of Fig. 4, we can see that the over all structure of the results is same but there is a dramatic change in the heights of the slow and fast shocks. Also we can see an increase in the minimum and maximum values of the y -component of velocity. Again the good performance of our codes shows the robustness and accuracy of the schemes.

7. Conclusions

In this paper we have constructed a BGK-type KFVS scheme for the SRMHD equations. The numerical flux function is constructed with consideration of particle transport across the cell interface and particle “collisions” are implemented in the transport process to reduce the numerical dissipation, especially at the contact discontinuity. The parameter χ , which determines the weights between the free transport and equilibrium fluxes, takes constant values in the current study.

Since in the 1D SRMHD case the solenoidal constraint $\nabla \cdot \mathbf{B} = 0$ is automatically satisfied and the transverse magnetic field components behave essentially like the other conservative variables, we can directly apply the schemes as the black-box solvers. Thus the 1D SRMHD system is composed of seven equations for the conserved variables in each direction. Due to the simplified nature of the relativistic kinetic phase density in the ultra-relativistic limit, and due to the reason that the normalization factor drops out in the split moment integrals for the velocity, we were able to use it for the splitting of the fluxes in SRMHD and URMHD equations in a unified way. The results obtained were also compared with the well developed central schemes. These central schemes are black-box, Jacobian-free MHD solvers whose sole input is the computed MHD fluxes. Despite of their simplicity these central schemes are able to resolve accurately the complex structure of 1D waves. All the test cases presented in this paper are very hard tests for the validity of both methods due to the presence of high shock gradients and relativistic effects in the simulations. Furthermore, we do not need to solve any complicated Riemann solver which is usually needed in most of the shock capturing upwind schemes. It was found that both kinetic and central schemes give comparable accuracy to the already published results in [6,36]. Although the results obtained from the upwind schemes are still better in accuracy, however the schemes we are using here have less computational cost. Both schemes are robust, compact and easy to implement on computer. The main advantage of the kinetic schemes over other schemes is that kinetic schemes ensures the positivity of pressure and energy density. Also the kinetic approach is more related to the physics of the given PDE system. In this study we have only investigated the 1D relativistic MHD equations. However, work is in progress to extend the schemes to the 2D case.

Acknowledgment

This research was supported by the German Research Foundation under DFG Contract Nos. WA633/6-3 and WA633/10-3.

Appendix A. Reduction of the volume integrals

Here we apply an important simplification to the volume integrals (10) and (11). We can see in (9) that the fields $\rho(t, \mathbf{x})$, $p(t, \mathbf{x})$, $e(t, \mathbf{x})$, and $\mathbf{v}(t, \mathbf{x})$ are not depending on $|\mathbf{q}|$. This fact enables us to reduce the three-fold volume integrals to twofold surface integrals by applying polar coordinates, see [18,20] for more details. Now using the relation

$$\int_{\mathbb{R}^3} f(|\mathbf{q}|) d^3q = \oint_{\partial B(0,1)} \int_0^\infty r^2 f(r) dr, \quad (\text{A.1})$$

one get the following reduced surface integrals from the volume moment integrals (10) and (11). For abbreviation we introduce the unit vector $\mathbf{n} = \mathbf{q}/|\mathbf{q}|$, then we have

$$N^\mu(t, \mathbf{x}) = \frac{1}{4\pi} \oint_{\partial B(0,1)} \frac{n^\mu \rho(t, \mathbf{x})}{\gamma^3(1 - \mathbf{n} \cdot \mathbf{v}(t, \mathbf{x}))^3} dS(\mathbf{n}), \quad (\text{A.2})$$

$$T^{\mu\nu}(t, \mathbf{x}) = \frac{3}{4\pi} \oint_{\partial B(0,1)} \left(\frac{n^\mu n^\nu (e + p)(t, \mathbf{x})}{\gamma^4(1 - \mathbf{n} \cdot \mathbf{v}(t, \mathbf{x}))^4} - \frac{1}{6} \frac{\rho \lambda(t, \mathbf{x}) g^{\mu\nu} \delta(e, p)}{\gamma^2(1 - \mathbf{n} \cdot \mathbf{v}(t, \mathbf{x}))^2} \right) dS(\mathbf{n}). \quad (\text{A.3})$$

Similarly one can easily see that

$$\rho(t, \mathbf{x}) = \frac{2}{\lambda} \int_{\mathbb{R}^3} f(t, \mathbf{x}, \mathbf{q}) \frac{d^3q}{|\mathbf{q}|} = \frac{1}{4\pi} \oint_{\partial B(0,1)} \frac{\rho(t, \mathbf{x})}{\gamma^2(1 - \mathbf{n} \cdot \mathbf{v}(t, \mathbf{x}))^2} dS(\mathbf{n}). \quad (\text{A.4})$$

Here $\mathbf{n} = \mathbf{q}/|\mathbf{q}|$ is the unit vector in direction of \mathbf{q} and $B(\mathbf{x}_0, r)$ is the ball with radius r and center \mathbf{x}_0 with boundary $\partial B(\mathbf{x}_0, r)$. Note that n^μ is not a four-vector and $n^0 = 1$.

References

- [1] M. Anile, *Relativistic Fluids and Magneto-fluids*, Cambridge University Press, Cambridge, MA, 1989.
- [2] M. Anile, S. Pennisi, Fluid models for relativistic electron beams, *Continuum Mech. Thermodyn.* 1 (1989) 267–282.
- [3] M. Abramowitz, I.A. Stegun, *Handbook of Mathematical Functions with Formulas, Graphs, and Mathematical Tables*, Dover, New York, 1965.
- [4] M.A. Aloy, J.M^a. Ibáñez, J.M^a. Martí, E. Müller, GENESIS: A high-resolution code for 3D relativistic hydrodynamics, *Astrophys. J.* 122 (1999) 151–166.
- [5] D. Balsara, Divergence free adaptive mesh refinement for magneto-hydrodynamics, *J. Comput. Phys.* 174 (2001) 614–648.
- [6] D. Balsara, Total variation diminishing scheme for relativistic magneto-hydrodynamics, *Astrophys. J., Suppl. Ser.* 132 (2001) 83–101.
- [7] D. Balsara, Second order accurate schemes for magnetohydrodynamics with divergence-free reconstruction, *Astrophys. J., Suppl. Ser.* 151 (2004) 149–184.
- [8] M.C. Begelman, R.D. Blandford, M.J. Rees, Theory of extragalactic radio sources, *Rev. Mod. Phys.* 56 (1984) 255–351.
- [9] M. Brio, C.C. Wu, An upwind differencing scheme for the equations of ideal magnetohydrodynamics, *J. Comput. Phys.* 75 (1988) 400–422.

- [10] J.-p. Croisille, R. Khanfir, G. Chanteur, Numerical simulation of the MHD equations by kinetic-type method, *J. Sci. Comput.* 10 (1995) 81–92.
- [11] W. Dai, P.R. Woodward, Extension of the piecewise parabolic method to multidimensional ideal magnetohydrodynamics, *J. Comput. Phys.* 115 (1994) 485–514.
- [12] C. DeVore, Flux-corrected transport techniques for multidimensional compressible magnetohydrodynamics, *J. Comput. Phys.* 92 (1991) 142–160.
- [13] R. Donat, A. Marquina, Capturing shock reflections: an improved flux formula, *J. Comput. Phys.* 125 (1996) 42–58.
- [14] F. Eulderink, G. Mellema, General relativistic hydrodynamics with a Roe solver, *Astron. Astrophys. Suppl.* 110 (1995) 587–623.
- [15] C.R. Evans, J.F. Hawley, Simulation of general relativistic magnetohydrodynamic flows: a constrained transport method, *Astrophys. J.* 332 (1988) 659.
- [16] A. Jameson, W. Schmidt, E. Turkel, Numerical solutions of the Euler equations by finite volume methods using Runge–Kutta time-stepping scheme AIAA81-1259, 1981.
- [17] F. Jüttner, Das Maxwell'sche Gesetz der Geschwindigkeitsverteilung in der Relativtheorie, *Ann. Phys. (Leipzig)* 34 (1911) 856–882.
- [18] M. Kunik, S. Qamar, G. Warnecke, Kinetic schemes for the ultra-relativistic Euler equations, *J. Comput. Phys.* 187 (2003) 572–596.
- [19] M. Kunik, S. Qamar, G. Warnecke, Kinetic schemes for the relativistic gas dynamics, *Numer. Math.* 97 (2004) 159–191.
- [20] M. Kunik, S. Qamar, G. Warnecke, A BGK-type kinetic flux-vector splitting schemes for the ultra-relativistic gas dynamics, *J. Sci. Comput.* 26 (2004) 196–223.
- [21] L.D. Landau, E.M. Lifshitz, *Fluid Mechanics*, Pergamon Press, New York, 1987.
- [22] A. Lichnerowicz, *Relativistic Hydrodynamics and Magnetohydrodynamics*, Benjamin, New York, 1967.
- [23] P. Londrillo, L. Del Zanna, High order upwind schemes for multidimensional magnetohydrodynamics, *Astrophys. J.* 530 (2000) 508.
- [24] J.M^a. Martí, E. Müller, J.A. Font, J.M^a. Ibáñez, Morphology and dynamics of highly supersonic relativistic jets, *Astrophysics. J.* 448 (1995) L105–L108.
- [25] J.M^a. Martí, E. Müller, Numerical hydrodynamics in special relativity, *Living Rev. Relat.* 2 (1999) 1–101.
- [26] I.F. Mirabel, L.F. Rodríguez, A superluminal source in the galaxy, *Nature* 371 (1994) 46.
- [27] P. Mészáros, M.J. Rees, Tidal heating and mass loss in neutron star binaries-implications for gamma-ray burst models, *APJ* 397 (1992) 570–575.
- [28] H. Nessyahu, E. Tadmor, Nonoscillatory central differencing for hyperbolic conservation laws, *SIAM J. Comput. Phys.* 87 (1990) 408–448.
- [29] P.L. Roe, D.S. Balsara, Notes on the eigensystem of magneto-hydrodynamics, *SIAM J. Appl. Math.* 56 (1996) 57–67.
- [30] D. Ryu, F. Miniati, T.W. Jones, A. Frank, A divergence-free upwind code for multidimensional magnetohydrodynamics flows, *Astrophys. J.* 509 (1998) 244–255.
- [31] V. Schneider, U. Katscher, D.H. Rischke, B. Waldhauser, J.A. Maruhn, C.-D. Munz, New algorithms for ultra-relativistic numerical hydrodynamics, *J. Comput. Phys.* 105 (1993) 92–107.
- [32] J.M. Stone, M.L. Norman, A radiation magnetohydrodynamics code for astrophysical flows in two space dimensions. II. The magnetohydrodynamic algorithms and tests, *APJ* 80 (1992) 791–818.
- [33] T. Tang, K. Xu, A high-order gas-kinetic method for multidimensional ideal magnetohydrodynamics, *J. Comput. Phys.* 165 (2000) 69–88.
- [34] K. Xu, Gas-kinetic theory based flux splitting method for ideal magneto-hydrodynamics, *J. Comput. Phys.* 153 (1999) 334–352.
- [35] L. Del Zanna, N. Bucciantini, An efficient shock-capturing central-type scheme for multidimensional relativistic flows, I. Hydrodynamics, *A&A* 390 (2002) 1177–1186.
- [36] L. Del Zanna, N. Bucciantini, P. Londrillo, An efficient shock-capturing central-type scheme for multidimensional relativistic flows, II. Magnetohydrodynamics, *A&A* 397 (2003) 397–413.